

# Noncollinear second-harmonic generation in sub-micrometer-poled RbTiOPO<sub>4</sub>

S. Moscovich, A. Arie, R. Urneski, A. Agronin, G. Rosenman AND Y. Rosenwaks

*Dept. of Electrical Engineering – Physical Electronics, Faculty of Engineering, Tel Aviv University,*

*Tel-Aviv 69978, Israel*

[ady@eng.tau.ac.il](mailto:ady@eng.tau.ac.il)

**Abstract:** We have generated noncollinear quasi-phase-matched second harmonic wave in an RbTiOPO<sub>4</sub> crystal that was poled using the high-voltage atomic force microscope (HV-AFM). To the best of our knowledge, this is the first systematic nonlinear frequency conversion study of samples produced by the HV-AFM method. The short poling period of 1.18  $\mu\text{m}$  enabled us to observe second harmonic generation at very large angles with respect to the fundamental wave. The setup was used to optically explore the homogeneity of the poled area. The measurements are in a reasonable agreement with an analytic calculations.

© 2004 Optical Society of America

OCIS codes: (190.0190) Nonlinear Optics; (190.2620) Frequency Conversion.

---

## References and Links

1. G. Rosenman, P. Urenski, A. Agronin, Y. Rosenwaks, and M. Molotskii, "Submicron ferroelectric domain structures tailored by high-voltage scanning-probe microscopy," *Appl. Phys. Lett.* **82**, 103-105, (2003).
2. C. Canalias, V. Pasiskevicius, R. Clemens, and F. Laurell, "Submicron periodically poled flux-grown KTiOPO<sub>4</sub>," *Appl. Phys. Lett.* **82**, 4233-4235 (2003).
3. S. E. Harris, "Proposed backward wave oscillations in the infrared," *Appl. Phys. Lett.* **9**, 114-116 (1966).
4. Y. J. Ding, J. U. Kang, and J. Khurgin, "Theory of backward second-harmonic and third-harmonic generation using laser pulses in quasi-phase-matched second order nonlinear medium," *IEEE J. Quantum Electron.* **34**, 966-974 (1998).
5. J. A. Giordmaine, "Mixing of light beams in crystals," *Physical Review Letters* **8**, 19-21 (1962).
6. Y. S. Oseledchik, A. I. Pisarevsky, A. L. Prosvirnin, V. V. Starshenko, and N. V. Svitanko, "Nonlinear optical properties of the flux grown RbTiOPO<sub>4</sub> crystal," *Opt. Mat.* **3**, 237-242 (1994).
7. G. Rosenman, P. Urenski, A. Agronin, A. Arie, and Y. Rosenwaks, "Nanodomain engineering in RbTiOPO<sub>4</sub> ferroelectric crystals," *Appl. Phys. Lett.* **82**, 3934-3936 (2003).
8. V. Berger, "Nonlinear photonic crystals," *Physical Review Letters* **81**, 4136-4139 (1998).
9. G. D. Boyd and D. A. Kleinman, "Parametric interaction of focused Gaussian light beams," *J. Appl. Phys.* **39**, 3597-3639 (1968).
10. M. M. Fejer, G. A. Magel, D. H. Jundt, and R. L. Byer, "Quasi-phase-matched second harmonic generation: tuning and tolerances," *IEEE J. Quantum Electron.* **28**, 2631-2654 (1992).
11. Raicol Crystals Ltd., P.O. Box 2753 Yehud, Israel.

---

## 1. Introduction

It was recently shown that by applying high voltage through the tip of an atomic force microscope [1], it is possible to periodically-pole ferroelectric crystals with sub-micrometer resolution. Furthermore, submicrometer poling was also demonstrated recently using electron-beam lithography techniques [2]. This represents nearly an order of magnitude improvement in poling resolution with respect to the commonly used technique of electric field poling. The improvement in poling periods opens new possibilities for quasi-phase-matched nonlinear optics, such as backward generating devices, e.g. backward optical parametric oscillator [3] and backward frequency doubler [4], as well as noncollinear frequency conversion [5] with large angles between the interacting waves. These nonlinear processes can also be used to characterize the new technique and the samples that can be produced by it.

Samples that were poled by the high-voltage atomic force microscope (HV-AFM) poling method have been characterized so far only by topographic scans using an atomic force microscope. However, the suitability of this poling method for nonlinear optics applications can only be verified by direct frequency conversion measurement. As the poling periods can be extremely short, conventional forward collinear nonlinear frequency conversion is usually not applicable. For example, the shortest period that can be used in forward collinear second harmonic generation in RbTiOPO<sub>4</sub> (RTP) is around 3 μm (for doubling 800 nm pump into 400 nm, near the edge of the RTP transmission window [6]). On the other hand, the periods that are required for efficient backward second harmonic generation into visible wavelengths are still too short with respect to the available resolution of the HV-AFM method. For example, first order backward second harmonic generation of 827 nm light requires a period of 0.107 μm. The grating used in this work had a period of 1.18 μm and should be suitable only for 11<sup>th</sup> order backward frequency doubling [7]. The best possibility for nonlinear characterization of samples with periods in the range of 1 μm is by noncollinear second harmonic generation. The K vector diagram for noncollinear quasi-phase-matching is shown in the inset of Fig. 1. It enables second harmonic generation at several different angles, corresponding to different quasi-phase matching orders. Forward and backward collinear second harmonic generation can be considered as special cases where the angle between the pump and second harmonic is either 0 degrees or 180 degrees, respectively.

## 2. Experimental setup

Flux-grown RTP crystals (Raicol Crystals, Ltd, Israel) were cut normal to the polar axis and thinned down to 200 μm. The HV-AFM was based on a modification of the Autoprobe CP AFM (Veeco, Inc). The domain reversal was performed by applying a high dc voltage (650 V) to the scanning HV-AFM tip having a radius of curvature of 50 nm. The tip velocity was 30 μm/s. The fabricated domain grating comprised of 26 squares with 75×75 μm<sup>2</sup> area and had a total dimension of 1×0.15 mm<sup>2</sup>. Inspection of the fabricated domain grating, following chemical etching, using optical microscopy indicated that the reversed domains propagated smoothly without significant change in their width throughout the crystal thickness from the C<sup>+</sup> to the C<sup>-</sup> polar face.

The PPRTP sample enabled to generate noncollinear second harmonic wave, using the experimental setup shown in Fig. 1. The pump was generated by a Q-switched Nd:YLF laser (Lightwave Electronics model 110-1047-50). The 1047.51 nm laser was operated at a repetition rate of 12.5 kHz, and the pulse energy and duration were 22 μJ and 9 ns, respectively. The laser beam was focused into the PPRTP sample, which was mounted on a rotation stage. Taking into account the losses in the optical setup and in the uncoated surface of the PPRTP crystal, the pump pulse energy in the crystal was ~ 9 μJ.

As the crystal was rotated, we have observed several distinct angles in which the second harmonic light was generated at relatively high efficiency. These angles correspond to different orders of noncollinear quasi-phase-matching in the crystal. At each one of these angles we have measured the second harmonic power (which was separated from the residual fundamental wave by several IR cut filters) using a Si photodetector. The angles of the fundamental and second harmonic waves in the different QPM orders are summarized in Table 1. The measurements for m=8 were taken when the laser beam entered the RTP sample through the surface that was perpendicular to the grating vector, whereas the other measurements for m=1, 2, 3 were made when the beam entered in the non-conventional manner, through the surface that was parallel to the grating vector. In the first two orders, we have observed second harmonic waves emerging simultaneously in two different angles, denoted  $\theta_{2\omega^+}$  and  $\theta_{2\omega^-}$ , respectively. In the higher orders, the second harmonic beam was observed only in the positive direction. This phenomenon is further discussed below.

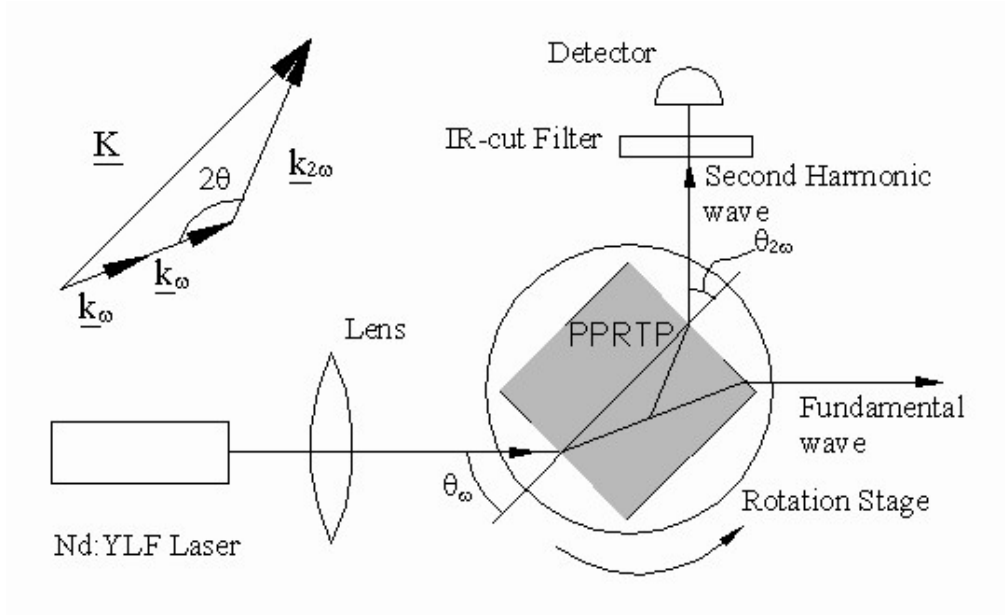


Fig. 1. Experimental setup for noncollinear second harmonic generation. Inset: K vector diagram for noncollinear second harmonic generation.

Table 1. Calculated and measured fundamental input angle and second harmonic output angle (both of them in air) for different QPM orders of noncollinear second harmonic generation. The angles are given in degrees.

Order m	Calculated		Measured		
	$\theta_\omega$	$\theta_{2\omega}$	$\theta_\omega$	$\theta_{2\omega}^+$	$\theta_{2\omega}^-$
1	3.09	29.85	3	30	32
2	17.8	35.57	18	35	34
3	35.02	49.26	35	48	-
8	39.68	39.68	40	39	-

### 3. Experimental results and analysis

Denoting the walk-off angle between the fundamental and second harmonic waves as  $2\theta$  (see Fig. 1), the noncollinear quasi phase matching relation is given by [8]:

$$\frac{\lambda_{2\omega}}{n_{2\omega}} = \frac{2\pi}{|G|} \sqrt{\left(1 - \frac{n_\omega}{n_{2\omega}}\right)^2 + 4 \frac{n_\omega}{n_{2\omega}} \sin^2 \theta}, \quad (1)$$

where  $\lambda_{2\omega}, n_{2\omega}$  are the wavelength and refractive index of the second harmonic wave,  $G = 2\pi m/\Lambda$ ,  $\Lambda$  is the poling period and  $n_\omega$  is the refractive index at the fundamental wavelength. Using Snell's law and the known refractive indices of the fundamental and

second harmonic waves in RTP, the angles in air  $\theta_\omega$  and  $\theta_{2\omega}$  can be calculated. As can be seen, the experimentally measured angles are in good agreement with the theoretical prediction.

The second harmonic power can be calculated analytically for an input Gaussian beam, assuming pump depletion can be neglected. This is a very reasonable assumption in our experiment, since the conversion efficiency is below  $10^{-3}$ . The second harmonic power is given by [9]:

$$P_{2\omega} = \frac{2\omega_1^2 d_{\text{eff}}^2 k_\omega}{\pi n_{2\omega}^2 \epsilon_0 c^3} L h P_\omega^2, \quad (2)$$

where  $\omega_1$ ,  $k_\omega$  are the angular frequency and wavevector of the fundamental beam, respectively,  $d_{\text{eff}}$  is the effective nonlinear coefficient,  $\epsilon_0$  and  $c$  are the free space permittivity and velocity of light in vacuum, respectively,  $L$  is the length of the periodically-poled region that the fundamental beam passes,  $h$  the focusing parameter of the beam and  $P_\omega$  the pump power.

The effective nonlinear coefficient of an ideal quasi-phase matched structure for  $m$ th order interaction is given by [10]

$$d_{\text{eff}} = \frac{2d_{33}}{\pi m}, \quad (3)$$

where  $d_{33}$  is the nonlinear coefficient for beams polarized in the  $z$  direction of the crystal (equal to 17.1 pm/V for RTP [11]).

Assuming that the absorption in the crystal is negligible and the beam is focused into the center of the interaction region, the optimal focusing parameter for the case of weak focusing can be approximated by:

$$h(B, \xi) \approx \xi G(2B\sqrt{2\xi}), \quad (4)$$

where  $B = \theta\sqrt{Lk_\omega}$  is the walk-off parameter,  $\xi$  is defined as the ratio between the crystal length  $L$  and the confocal parameter of the Gaussian beam, and the function  $G$  is given by

$$G(t) = \sqrt{\frac{2\pi}{t^2}} \text{erf}\left(\frac{t}{\sqrt{2}}\right) - \frac{2}{t^2} \left(1 - e^{-t^2/2}\right), \quad (5)$$

where erf is the Gaussian error function. Equation (4) is valid for  $\xi < 0.4$ , which is fulfilled for the experiments carried in this work. In this case, the expected second harmonic power for  $m$ th order quasi-phase-matched frequency doubling of Nd:YLF in RTP (in MKS units) is simply given by

$$P_{2\omega} \cong \frac{1.7LhP_\omega^2}{m^2}. \quad (6)$$

The beam waist that was used in our experiment was 35  $\mu\text{m}$ . The pump peak power in the crystal was in the range of 850-1050 W. The effective interaction length was determined by calculating the geometrical length that the fundamental beam passes in the periodically-poled area. The measured and calculated second harmonic conversion efficiencies in each order are given in Table 2. The measured efficiencies are about one sixth up to one half of the theoretically calculated power. This may be explained by random variations of the duty cycle

and period of the poled domain structure [10]. Since the second harmonic power strongly depends on the position of the beam in the crystal, the second harmonic power levels shown in Table 2 correspond to the highest efficiency locations.

Table 2. Calculated and measured frequency doubling efficiency, effective interaction length and measured peak second harmonic power for different QPM orders of noncollinear second harmonic generation.

m	$\eta_{\text{experiment}}$	$\eta_{\text{theory}}$	L [ $\mu\text{m}$ ]	$P_{2\omega}$ [mW]
1	4.94e-4	3e-3	150	518
2	1.44e-4	6.8e-4	152	145
3	6.37e-5	2.3e-4	158	54.8
8	4.3e-5	8.35e-5	329	38.2

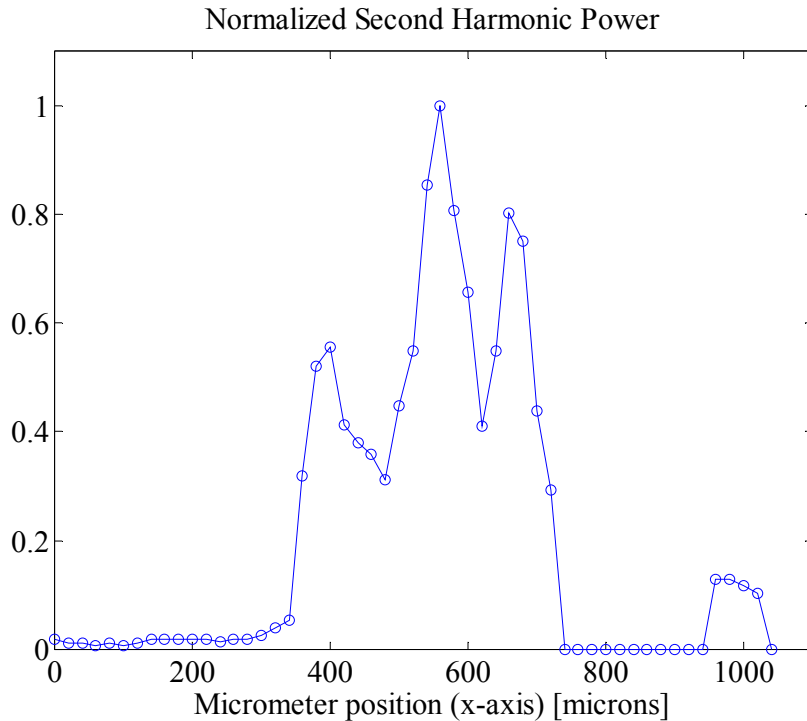


Fig. 2. Variation of the second harmonic power in 1<sup>st</sup> order QPM as the beam travels along the x-axis (length dimension) of the crystal.

The grating uniformity was evaluated by translating the crystal in the case of first order interaction (where the beam is almost perpendicular to the grating structure). The second harmonic power level varied significantly during the scan, see Fig. 2. We have observed 3 peaks of intensity in the central part of the poled area, and negligible efficiency in other parts of the crystal. The areas showing high conversion efficiency have a width of  $\sim 75 \mu\text{m}$  which corresponds to the area that was poled in a single step by the atomic force microscope. Apparently, the period is homogenous enough to provide high conversion efficiency in this area. However, the large variations in efficiency over larger areas indicate that the periodicity is not maintained with sufficient accuracy between adjacent  $75 \times 75 \mu\text{m}$  AFM pitches. In this sample, the translation between pitches was done using a manual translation stage. It seems

that a translation stage with higher accuracy, or a multiple tip array is required to ensure fixed poling period over large area.

We have also scanned the beam from the +C to the -C surface of the sample in order to evaluate the homogeneity of the sample in the Z direction, see Fig. 3. While the sample was 200  $\mu\text{m}$  thick, we have observed relatively high conversion efficiency in first order quasi-phase-matched frequency doubling only in the top  $\sim 100 \mu\text{m}$  (the reduced efficiency in the first  $\sim 70 \mu\text{m}$  is owing to the clipping of the beam by the crystal near the top surface). This may indicate that the duty cycle is not maintained throughout the entire thickness of the sample. Nevertheless, a 100  $\mu\text{m}$  thick poled area is of significance for various bulk optics devices.

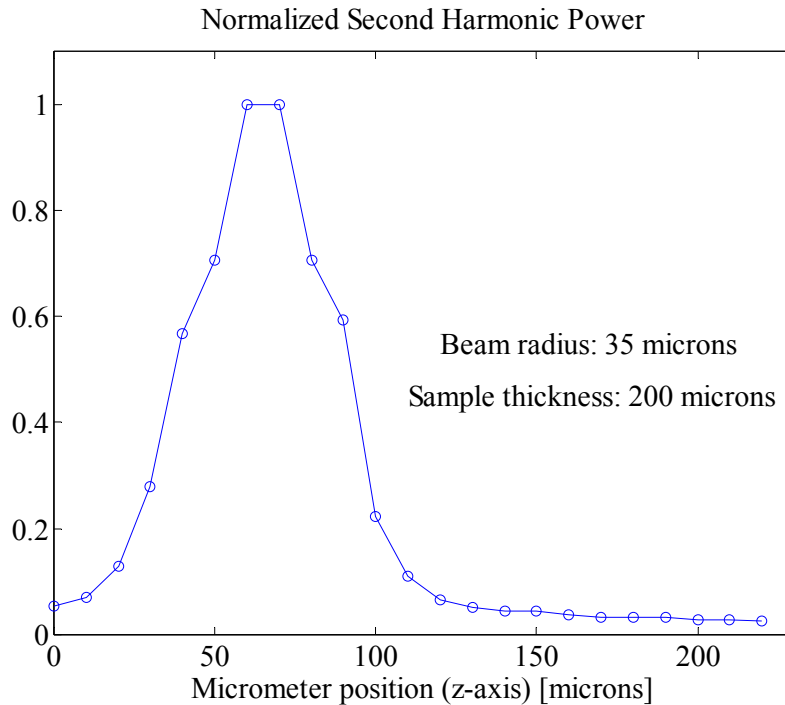


Fig. 3. Variation of the second harmonic power in 1<sup>st</sup> order QPM as the beam travels along the z-axis (thickness dimension) of the crystal.

It is interesting to note that in the first order and second order quasi-phase-matched interactions, we have observed second harmonic beams in both the positive and negative angles with respect to the grating wavevector, although the power level at the negative angle was always lower than that of the positive angle. At the higher orders of QPM, second harmonic light was observed only in the positive angles. This phenomenon can be explained using the following K-vector diagram (Fig. 4): Since the interacting waves are not collinear, usually only one direction is phase matched. However, when the fundamental beam is nearly perpendicular to the grating wave vector, then both the positive and negative angles are near phase matching. As the QPM order becomes higher, the difference between the phase mismatch of the positive and negative angles becomes more pronounced, and indeed for 3<sup>rd</sup> and 8<sup>th</sup> order QPM we have observed second harmonic wave only in the positive angles.

We have also characterized the sample using a different pump source – a high repetition rate Ti:Sapphire laser with psec pulses, operating near 840 nm. With this laser we have observed noncollinear frequency doubling at the first 5 QPM orders. At 11<sup>th</sup> QPM order the sample should produce second harmonic generation at the opposite direction to the input

pump [7]. However, we were unable to observe this backward conversion, apparently owing to the short length of the poled area and its high inhomogeneity.

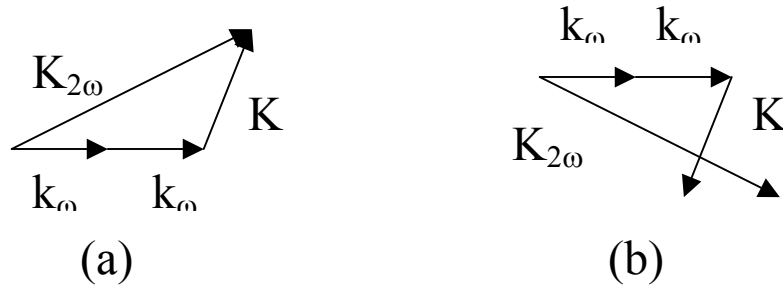


Fig. 4. K Vector diagram for positive and negative angles in noncollinear SHG: Phase matching is achieved for one direction of propagation (a), but not for the opposite direction (b).

#### 4. Summary

In summary, we have shown that densely-poled RTP crystals can be suitable for large-angle noncollinear quasi-phase-matched frequency conversion. Although there are large variations in the second harmonic efficiency, the results in areas of high efficiency are in good agreement with the theoretical predictions, thus indicating the potential of the HV-AFM technique for producing quasi-phase-matched nonlinear frequency mixers. Further improvement in the HV-AFM poling technique, e.g. using multiple tip array, may enable to pole larger areas and with improved homogeneity. This improvement may also enable to efficiently realize backward processes such as backward second harmonic generation and backward optical parametric oscillation.

#### Acknowledgment

This work was supported by the Israeli Ministry of Science.